

Numerical simulation of the plunge stage of friction surfacing of AA5083 aluminum alloy

Hongjun Li, Zhuang Xu, Zhewei Zhou,

Zhejiang Sci-Tech University, Hangzhou, 310018, China

E-mail: lihongjun@zstu.edu.cn

Abstract. Plunge stage is crucial to the success of whole friction surfacing process. To investigate the effect of parameters, the CEL modelling method in the finite element software model was used to simulate the plunge stage of friction surfacing. The results showed that the higher rotation speed would result a smaller axial force but higher the center point temperature and frictional dissipation; Besides, a higher feed rate, who can cause higher peek value of axial force and the center point temperature rises faster, is inversely proportional to the frictional dissipation, and the final axial force and the center point temperature tended to be in the same range.

1. Introduction

Friction surfacing is a solid phase joining technique that can be used to produce metal coatings. Schematic diagram of friction surfacing is shown in Figure 1. Under the axial force, the high-speed rotating consumable rod was rubbed against the substrate and the end of the consumable rod was heated. With the relative movement of the consumable rod and the substrate, the consumable rod was continuously transferred to the substrate to form a continuous deposited layer [1]. The welding process parameters, including the feed rate, the rotating speed and the welding speed would affect the thermal coupling between the surfacing layers, and consequently the welding quality of the surfacing layer [2].

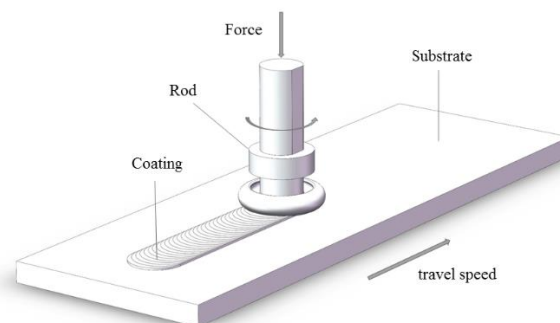


Figure 1. Schematic diagram of friction surfacing

At present, the research on the mechanism of friction surfacing is mainly based on deposition process of steel over steel [3-4], aluminum alloy over aluminum alloy [5-6], but there are few studies on aluminum/steel surfacing in the literature [7-11]. By means of numerical analysis, the material plastic deformation, temperature change of the consumable rod, formation mechanism of the deposited layer can be obtained. Liu et al. [12] applied the finite element method to the coupling calculation of the friction welding process. But due to the limitations of the Lagrangian method in dealing with large



Content from this work may be used under the terms of the [Creative Commons Attribution 3.0 licence](https://creativecommons.org/licenses/by/3.0/). Any further distribution of this work must maintain attribution to the author(s) and the title of the work, journal citation and DOI.

nonlinear deformation, it was impossible to simulate the stable surfacing stage. Other numerical simulation studies [13-15] only analyzed the temperature field using a simplified heat source model. So the simulation study of the surfacing process is still very scarce.

Deposition process of aluminum over steel has a wide range of requirements in shipbuilding, automotive and aerospace [16]. In this paper finite element software was used to establish a thermal mechanical coupled friction surfacing model and to simulate the compression stage and then to obtain the deformation of consumable rod in the compression stage.

2. Modelling

2.1 Model geometry

The consumable rod undergo large plastic deformation during the surfacing process, was defined as Eulerian body, and the substrate was defined as rigid body. The consumable rod was cylindrical, with diameters and heights of 20 mm and 100 mm, respectively. The Eulerian body included two regions, 'full' and 'void'. The outer region 'void' contained no initial AA5083 material properties. The substrate diameter and height are 15 mm and 3 mm. As shown in Figure 2 and 3:

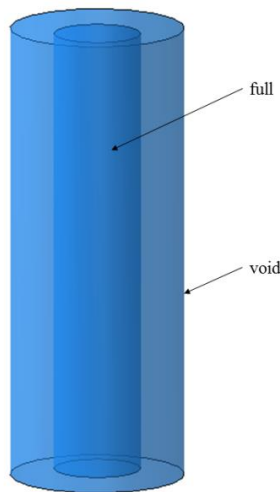


Figure 2. Rod geometrical model

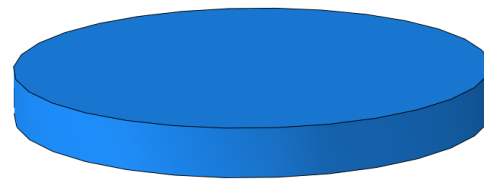


Figure 3. Substrate geometrical model

2.2 Material properties

The consumable rod are AA5083 aluminum alloy, that belongs to Al-Mg alloy, which has high strength, corrosion resistance and excellent welding performance [17]. The physical properties of AA5083 are shown in Tables 1:

Table 1. Temperature dependent properties of AA5083 steel [18]

Temperature (°C)	Thermal conductivity (W·m ⁻¹ ·K ⁻¹)	Specific heat capacity (J·Kg ⁻¹ ·°C ⁻¹)	Density (Kg·m ⁻³)
-20	112.5	924.1	2673.9
80	122.7	984.2	2642.7
180	131.6	1039.6	2629.4
280	142.3	1081.2	2611.5
380	152.5	1136.6	2589.3
480	159.5	1178.2	2567.0
580	177.2	1261.4	2549.2

The Johnson-Cook plasticity model was used in the finite element simulation of friction surfacing with high strain rate deformation [19]. The parameters of the AA5083 aluminum alloy Johnson-Cook are shown in Table 2:

Table 2. Johnson-Cook Plasticity Coefficients for AA5083 [20]

A(GPa)	B(GPa)	n	C	m	$T_m(^{\circ}\text{C})$	$T_r(^{\circ}\text{C})$
0.13789	0.21673	0.4845	0.002	1.225	660	20

2.3 Boundary conditions

The simulation mainly studied the influence of process parameters on the friction surfacing process. Since only the compression stage of the friction surfacing was simulated, the rotating speed and the feed rate were merely considered in the experiment. Five sets of simulated parameters were tested, and the feed was 7 mm. The specific process parameters were shown in Table 3:

Table 3. Process parameters of simulation

Test	Rotating speed ($\text{r}\cdot\text{min}^{-1}$)	Feed rate ($\text{mm}\cdot\text{min}^{-1}$)
1	700	20
2	900	20
3	1100	20
4	900	15
5	900	25

3. Results and discussion

3.1 Axial force

When the feed rate was 20 mm/min, the effects of the rotational speeds of 700, 900 and 1100 r/min on the axial force P are shown in Figure 4. Due to the instability of plastic deformation during frictional surfacing. The axial force was in a fluctuating state. The higher the rotational speed, the more heat was generated by the consumable rod, and the material at the bottom of the consumable rod was more softer, so the lower the axial force; when the rotation speed was 900r/min, the influence of the feed rate of 15, 20 and 25 mm/min on the axial force is shown in Figure 5. The peak value of the axial force P_{\max} (25 mm/min) $>$ P_{\max} (20 mm/min) $>$ P_{\max} (15 mm/min), but when the surfacing is carried out, the downforce tended to be in the same range.

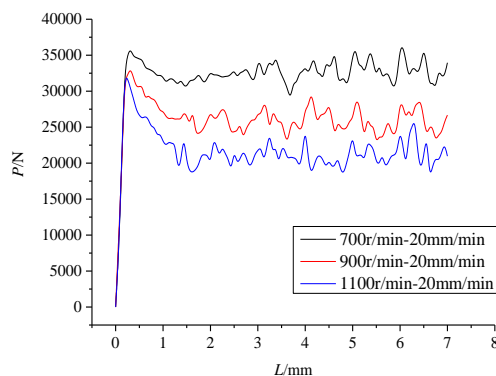


Figure 4. Effect of rotational speed on axial force

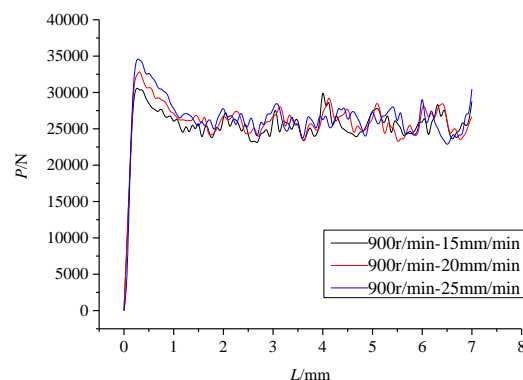


Figure 5. Effect of feed rate on axial force

3.2 Temperature of the center point of the contact surface

When the feed rate was 20 mm/min, the effects of the rotational speeds of 700, 900 and 1100 r/min on the contact point center temperature are shown in Figure 6. The higher the speed, the higher the center point temperature rises fast, and the center point temperature $T(1100 \text{ r/min}) > T(900 \text{ r/min}) > T(700 \text{ r/min})$, when the rotation speed was 900 r/min, the feed rate was 15, 20 and 25 mm/min on the center point temperature is shown in Figure 7. The faster the feed rate, the more friction between the consumable rod and the substrate, the faster the temperature rises at the center point, and due to the same displacement, the center point temperature tended to be in the same range as the friction surfacing continued.

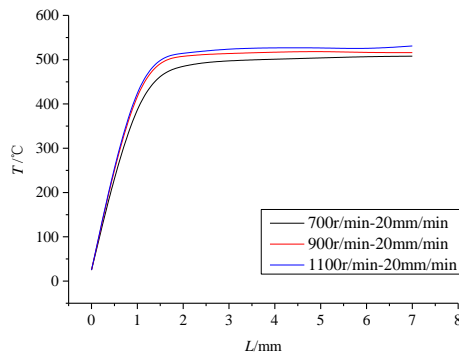


Figure 6. Effect of rotational speed on temperature

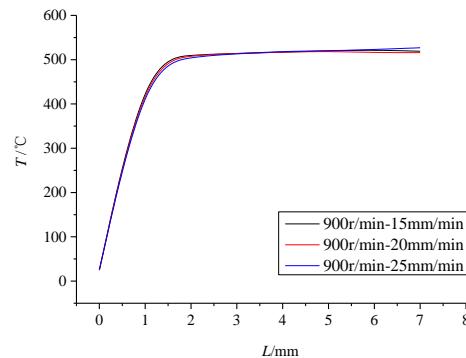


Figure 7. Effect of feed rate on temperature

3.3 Frictional dissipation

When the feed rate was 20mm/min, the effects of the rotational speeds of 700, 900 and 1100 r/min on the material frictional dissipation Q_f are shown in Figure 8. The higher the rotation speed, the greater the frictional dissipation. When the rotation speed was 900 r/min, the effect of the feed rate of 15, 20 and 25 mm/min on Q_f is shown in Figure 9. The higher the feed rate, the shorter friction surfacing time and the smaller the frictional dissipation.

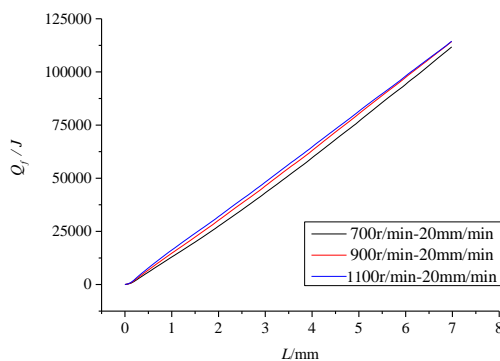


Figure 8. Effect of rotational speed on frictional dissipation

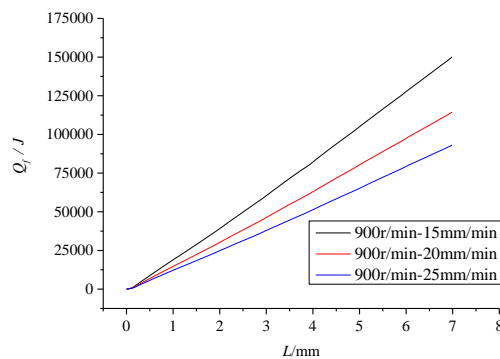


Figure 9. Effect of feed rate on frictional dissipation

4. Conclusions

- 1) The higher the rotation speed, the smaller the axial force; the higher the feed rate, the greater the peak value reached, but eventually axial force tended to be in the same range.
- 2) The higher the rotation speed, the higher the center point temperature; the higher the feed rate, the faster the center point temperature rises, but finally center point temperature tended to be in the same range.

- 3) The higher the rotation speed, the greater the frictional dissipation; the higher the feed rate, the smaller the frictional dissipation.

References

- [1] Badheka K and Badheka V 2017 Friction surfacing of aluminium on steel: An experimental approach *Materials Today: Proceedings* **4**(9) pp 9937-9941
- [2] Padhy G K, Wu C S and Gao S 2018 Friction stir based welding and processing technologies-processes, parameters, microstructures and applications: A review *Journal of Materials Science & Technology* **34**(1) pp 1-38
- [3] Rafi H K, Ram G D J, Phanikumar G, Rao and K P 2011 Microstructural evolution during friction surfacing of tool steel H13 *Materials & Design* **32**(1) pp 82-87
- [4] George S N R, Mohanty B S and Sathish R 2018 Friction surfacing of AISI 316 over mild steel: A characteriation study. *Defence Technology* **14**(4) pp 306-312
- [5] Galvis J C, Oliveira P H F, Hupaló M F, Martins J P and Carvalho A L M 2017 Influence of friction surfacing process parameters to deposit AA6351-T6 over AA5052-H32 using conventional milling machine *Journal of Materials Processing Technology* **245** pp 91-105
- [6] Krohn H, Hanke S, Beyer M and Dos Santos J F 2015 Influence of external cooling configuration on friction surfacing of AA6082 T6 over AA2024 T351 *Manufacturing Letters* **5** pp 17-20
- [7] Chandrasekaran M, Batchelor A W and Jana S 1997 Friction surfacing of metal coatings on steel and aluminum substrate *Journal of Materials Processing Technology* **72**(3) pp 446-452
- [8] Li, H.; Qin, W.; Galloway, A.; Toumpis, A. 2019 Friction Surfacing of Aluminium Alloy 5083 on DH36 Steel Plate. *Metals*, **9**, 479
- [9] Sugandhi V and Ravishankar V 2012 Optimization of friction surfacing process parameters for aa1100 aluminum alloy coating with mild steel substrate using response surface methodology (RSM) technique *Modern Applied Science* **6** pp 69-80
- [10] Badheka K and Badheka V 2017 Friction Surfacing of Aluminium on Steel: An Experimental Approach *Materials Today: Proceedings* **4**(9) pp 9937-9941
- [11] Kumar B V, Reddy G M and Mohandas T 2015 Influence of process parameters on physical dimensions of AA6063 aluminium alloy coating on mild steel in friction surfacing *Defence Technology* **11**(3) pp 275-281
- [12] Liu X M, Zou Z D, Zhang Y H, Qu S Y and Wang X H 2008 Transferring mechanism of the coating rod in friction surfacing *Surface & Coatings Technology* **202**(9) pp 1889-1894
- [13] Liu X, Yao J, Wang X, Zou Z and Qu S 2009 Finite difference modeling on the temperature field of consumable-rod in friction surfacing *Journal of Materials Processing Technology* **209**(3) pp 1392-1399
- [14] Vitanov V I and Javaid N 2010 Investigation of the thermal field in micro friction surfacing *Surface & Coatings Technology* **204**(16) pp 2624-2631
- [15] Jaworski B, Voutchkov I I, Vitanov V I and Hughes V 2000 Modelling of the friction surfacing process for turbine blade reclamation *Proceedings of the 33rd International MATADOR Conference* Springer London pp 307-312
- [16] Ravisekhar S, Das V C and Govardhan D 2017 Friction surfaced deposits for industrial applications *Materials Today: Proceedings* **4**(2) pp 3796-3801
- [17] Ahmad B, Galloway A and Toumpis A 2018 Advanced numerical modelling of friction stir welded low alloy steel *Journal of Manufacturing Processes* **34** pp 625-636
- [18] Gupta M S N, Balunaik B and Murti K G K 2012 Finite element modeling and thermo-mechanical analysis of friction stir welded Al/Cu bimetallic lap joints *International Journal of Mechanical Engineering and Robotics Research* **2**(17) pp 165-173
- [19] Johnson GR and Cook WH 1983 A constitutive model and data for metals subject to large strains, strain rates and high temperature. In: proceedings of 7th Int. Sym. Ballistics, Editors. Seventh International Symposium on Ballistics Hague-Netherlands pp 541-547
- [20] Polyzois I and Polyzois I 2010 Finite element modeling of the behavior of armor materials under high strain rates and large strains